J Therm Anal Calorim (2012) 109:1095–1103
DOI 10.1007/s10973-011-2125-1

Prediction of thermal hazard of liquid organic peroxides by non-isothermal and isothermal kinetic model of DSC tests

Jo-Ming Tseng · Tung-Feng Hsieh · Yi-Ming Chang · Ya-Chen Yang · Lu-Yen Chen · Chun-Ping Lin

NATAS2011 Conference Special Chapter

Abstract Liquid organic peroxides (LOPs) have been widely used as initiators of polymerization, hardening, or cross-linking agents. We evaluated a beneficial kinetic model to acquire accurate thermokinetic parameters to help preventing runaway reactions, fires or explosions in the process environment. Differential scanning calorimetry was used to assess the kinetic parameters, such as kinetic model, reaction order, heat of reaction (ΔH_d), activation energy (E_a), frequency factor ($\ln k_0$), etc. The non-isothermal and isothermal kinetic models were compared to determine the validity of the kinetic model, and then applied to the thermal hazard assessment of commercial package contaminated with LOPs. Simulations of a 0.5-L Dewar vessel and 25-kg commercial package were performed. We focused on the thermal stability of different liquid system properties for LOPs. From the results, the optimal conditions were determined for avoiding violent heat effects that can cause a runaway reaction in storage, transportation, and manufacturing.

J.-M. Tseng
Institute of Safety and Disaster Prevention Technology, Central Taiwan University of Science and Technology, 666, Buzih Rd., Taichung 40601, Taiwan, ROC

T.-F. Hsieh · Y.-M. Chang
General Education Center, Chienkuo Technology University, 1, Chieh Shou N. Rd., Changhua 50094, Taiwan, ROC

Y.-C. Yang · C.-P. Lin (✉)
Department of Health and Nutrition Biotechnology, Asia University, 500, Lioufeng Rd., Wufeng, Taichung 41354, Taiwan, ROC
e-mail: chunping927@gmail.com; cp.lin@asia.edu.tw

L.-Y. Chen
Department of Emergency and Resources, National United University, 1, Lienda Rd., Miaoli 36003, Taiwan, ROC

Keywords Liquid organic peroxides · Differential scanning calorimetry · Non-isothermal kinetic model · Isothermal kinetic model · Simulation

List of symbols

C_P	Specific heat capacity (J g^{-1} K^{-1})
CT	Control temperature (°C)
E_a	Activation energy (kJ mol^{-1})
E_1	Activation energy of the 1st stage (kJ mol^{-1})
E_2	Activation energy of the 2nd stage (kJ mol^{-1})
ET	Emergency temperature (°C)
f_i	Kinetic functions of the ith stage $i = 1, 2, 3$
$f(\alpha)$	Kinetic functions
k_0	Pre-exponential factor (m^3 mol^{-1} s^{-1})
k_i	Reaction rate constant (mol L^{-1} s^{-1}) $i = 1, 2$
n	Reaction order or unit outer normal on the boundary, dimensionless
NC	Number of components, dimensionless
n_i	Reaction order of the ith stage, dimensionless $i = 1, 2, 3$
Q_i^∞	Specific heat effect of a reaction (J kg^{-1})
q	Heat flow (J g^{-1})
R	Gas constant (8.31415 J K^{-1} mol^{-1})
r_i	Reaction rate of the ith stage (g sec^{-1}) $i = 1, 2, 3, 4$
S	Heat-exchange surface (m^2)
SADT	Self-accelerating decomposition temperature (°C)
T	Absolute temperature (K)
T_0	Exothermic onset temperature (°C)
TCL	Time to conversion limit (year)
TCR	Critical temperature (°C)
TER	Total energy release (kJ kg^{-1})
T_e	Ambient temperature (°C)
TMR_{iso}	Time to maximum rate under isothermal conditions (day)

T_{wall}	Temperature on the wall (°C)
t	Time (sec)
W	Heat power (W g^{-1})
z	Autocatalytic constant, dimensionless
α	Degree of conversion, dimensionless
γ	Degree of conversion, dimensionless
ρ	Density (kg m^{-3})
λ	Heat conductivity (W m^{-1} K^{-1})
χ	Heat transfer coefficient (W m^{-2} K^{-1})
ΔH_d	Heat of decomposition (kJ kg^{-1})

Introduction

Liquid organic peroxides (LOPs), which have been widely employed in the chemical industry, are used to manufacture polymer materials. Tert-butyl hydroperoxide (TBHP) and tert-butyl (2-ethylhexyl) monoperoxy carbonate (TBEC) are commercial liquid organic peroxides which are to be transported and stored under limited temperature [1–5]. In terms of manufacturing and international management, many serious explosions and high ambient temperature occur because of thermal decomposition [1–5].

In particular, TBHP and TBEC are different LOPs: one is a solution, and the other is inherently liquid under room temperature. This study focused on the thermal stabilities of different liquid system properties for LOPs. They also are very dangerous goods for process manufacturing and stored management. This study will show how to obtain unknown LOPs by simple differential scanning calorimetry (DSC) tests and swift thermal analysis technology.

Comparisons of non-isothermal and isothermal kinetic models simulations led to a beneficial kinetic model of thermal decomposition to predict the thermal hazard of LOPs. The chosen approach was to establish an effective model of the thermal decomposition that included the kinetic parameters and thermal reactivity properties [6–8], such as the kinetics of reaction, pre-exponential factor ($\ln k_0$), reaction order (n), activation energy (E_a), heat of decomposition (ΔH_d), isothermal time to maximum rate (TMR_{iso}), time to conversion limit (TCL), and total energy release (TER), etc. In, addition, the kinetic parameters and thermal reactivity properties of LOPs could be applied as a reduction of energy potential, and safer design during relevant operations and storage conditions. This study acquired thermal decomposition properties, such as $\ln(k_0)$, reaction order (n), E_a, TMR_{iso}, TCL, TER, and ΔH_d by thermal hazard assessment software. DSC experimental data were processed and then the kinetics was evaluated by applying simulation [6–8].

Our aim was to develop a simple and swift green technology that could replace the complex tests by the traditional self-accelerating decomposition temperature (SADT) tests. The chosen approach was to establish a procedure for liquid thermal explosion assessment that included the safety parameters [9–21], such as the SADT, control temperature (CT), emergency temperature (ET), and the critical temperature (TCR), for a container or reactor containing LOPs. The method for estimation of the liquid thermal explosion parameters based on the Frank–Kamenetskii theory is well recognized [22]. Analytical evaluations of the critical conditions are also known for containers of the simplest form and constant boundary conditions of the first, second and third kind. For containers of complex form consisting of elements with various thermophysical properties, it may be rather difficult to obtain analytical evaluations [9, 10].

Therefore, the study was applied to simulate 0.5-L and 25-kg containers with the aim of developing a reliable procedure to replace the complex method for evaluating the thermokinetic parameters and predicting the thermal hazard of LOPs. The model may be applied to the optimal conditions to avoid LOPs' violent runaway reactions during manufacturing, storage, and transportation.

Experimental and method

Samples

TBHP 70 mass% solution and TBEC 95 mass% liquid, which were supplied directly from ACE Chemical Corp in Taiwan, were stored in a refrigerator at 4 °C. Experiments involved DSC non-isothermal tests at various scanning rates of 1, 2, 4, and 6 °C min^{-1}. DSC isothermal tests were held at conditions of 125–140 and 120–135 °C, for TBHP and TBEC, respectively.

Differential scanning calorimetry

Temperature-programmed screening experiments were performed with DSC (TA Q20). The test cell was used to carry out the experiment for withstanding relatively high pressure to approximately 10 MPa. ASTM E698 was used to obtain thermal curves for calculating kinetic parameters. Approximately 2–3 mg of the sample was used to acquire the experimental data. Non-isothermal tests of the scanning rate selected for the programmed temperature ramp were 1, 2, 4, and 6 °C min^{-1}. The range of temperature rise chosen was from 30 to 300 °C for each experiment. Several isothermal tests of the holding isothermal condition were performed at 125–140 and 120–135 °C, for TBHP and TBEC, respectively.

Liquid thermal hazard simulation

We used a 0.5-L Dewar vessel and a 25-kg commercial barrel package, as the reactor sizes to simulate the thermal hazard. The values of radius, height, of shell thickness and the reactors are listed in Table 1.

Results and discussion

Determination of thermokinetic parameters by DSC

Simulations of kinetic models can be complex multi-stage reactions that may consist of several independent, parallel, and consecutive stages [6–10]: Simple single-stage reaction:

$$\frac{d\alpha}{dt} = k_0 e^{\frac{-E_a}{RT}} f(\alpha) \quad (1)$$

Single-stage for nth order reaction:

$$\frac{d\alpha}{dt} = k_0 e^{\frac{-E_a}{RT}} (1-\alpha)^n \quad (2)$$

Multi-stage for autocatalytic reaction:

$$f(\alpha) = (1-\alpha)^{n_1}(\alpha^{n_2} + z) \quad (3)$$

where E_a is the activation energy, k_0 is the pre-exponential factor, z is the autocatalytic constant, and n_1 and n_2 are the reaction orders of a specific stage.

Reactions that include two consecutive stages:

$$\frac{d\alpha}{dt} = k_1 e^{\frac{-E_1}{RT}} (1-\alpha)^{n_1}; \frac{d\gamma}{dt} = k_2 e^{\frac{-E_2}{RT}} (\alpha-\gamma)^{n_2} \quad (4)$$

where α and γ are the conversions of the reactant A and product C, respectively. E_1 and E_2 are the activation energies of the stages.

Two parallel reactions for full autocatalysis:

$$\frac{d\alpha}{dt} = r_1(\alpha) + r_2(\alpha); \quad \begin{matrix} r_1(\alpha) = k_1(T)(1-\alpha)^{n_1} \\ r_2(\alpha) = k_2(T)\alpha^{n_2}(1-\alpha)^{n_3} \end{matrix} \quad (5)$$

where r_1 and r_2 are the rates of each stage, and n_3 is the reaction order of stage three.

The kinetic parameters were determined from the DSC experimental data at various scanning rates of 1, 2, 4, and 6 °C min^{-1}, isothermal tests holding isothermal conditions of 125–140 and 120–135 °C, for TBHP and TBEC, respectively, as displayed in Figs. 1 and 2, respectively. The experimental results of non-isothermal and isothermal of DSC tests are listed in Tables 2 and 3, respectively. The thermal decomposition of LOPs represents an unknown mechanism of reaction, such as an nth order or autocatalytic reaction. Here, using the nth order and autocatalytic simulations to calculate the thermokinetic parameters and then to compare the results of non-isothermal and isothermal of kinetic model simulation, we obtained the beneficial mechanism of thermal decomposition for LOPs. The simulation results are presented in Tables 4, 5, 6 and 7.

Tables 4, 5, 6 and 7 show that they can be matched very well to the results of the autocatalytic simulations and the

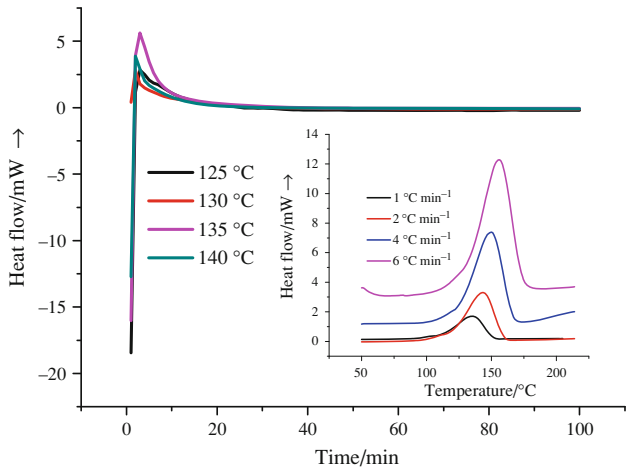

Fig. 1 DSC thermal curves of heat flow versus temperature for TBHP decomposition with scanning rates of 1, 2, 4, and 6 °C min^{-1} and with isothermal temperatures of 125, 130, 135, and 140 °C

Table 1 Boundary conditions for 0.5-L Dewar vessel and 25-kg barrel packages

Package shape	Size			Boundary conditions/ Initial temperature/°C		χ/W m^{-2}/K
	Radius/m	Height/m	Shell thickness/m			
0.5-L vessel	0.0285	0.18	0.00286	Top/3rd kind	20	1.4567[a]
				Side/3rd kind		1.4567[a]
				Bottom/1st kind		–
25-kg barrel	0.20	0.3	0.015	Top/3rd kind	20	2.8386[a]
				Sides/3rd kind		2.8386[a]
				Bottom/1st kind		–

[a] Yang et al. [20]

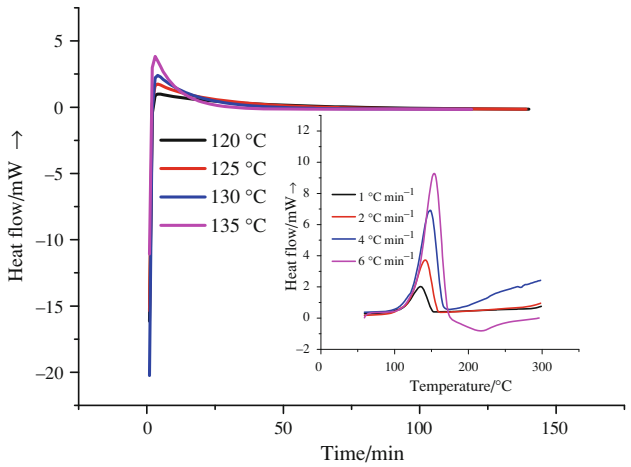

Fig. 2 DSC thermal curves of heat flow versus temperature for TBEC decomposition with scanning rates of 1, 2, 4, and 6 °C min^{-1} and with isothermal temperatures of 120, 125, 130, and 135 °C

Table 2 Results of DSC tests of TBHP and TBEC at various with scanning rates of 1, 2, 4, and 6 °C min^{-1}

Sample	Sample mass/mg	Scanning rate/°C/min	Onset temperature, T_o/°C	Peak of Temperature, T_p/°C	ΔH_d /kJ/kg
TBHP	2.8	1	110	135	883.6
	2.6	2	117	143	999.0
	3.3	4	123	149	746.2
	3.0	6	128	155	858.5
TBEC	3.0	1	111	135	843.6
	2.9	2	117	142	921.7
	3.0	4	122	148	876.2
	2.9	6	127	154	953.2

Standard deviation: temperature accuracy: ±0.1; temperature precision: ±0.05 calorimetric reproducibility: ±1%; sensitivity: 1.0 uW

Table 3 Results of DSC tests of TBHP and TBEC under different isothermal conditions

Sample	Sample mass/mg	Isothermal conditions/°C	ΔH_d//kJ/kg
TBHP	2.5	125	776.9
	2.3	130	708.3
	2.7	135	730.6
	2.3	140	718.6
TBEC	2.9	120	652.1
	3.3	125	697.8
	3.2	130	750.6
	3.0	135	622.0

Standard deviation: temperature accuracy: ±0.1; temperature precision: ±0.05 calorimetric reproducibility: ±1%; sensitivity: 1.0 uW

*n*th order simulation for TBHP and TBEC, respectively. Moreover, Tables 5 and 7 show the samples that were tested under the high isothermal conditions; the overheating effect was greater than non-isothermal DSC tests. Thus, the result of isothermal kinetic-model simulation was concerned with the overheating effect of the kinetic parameters and they were excluded from further analysis. Fortunately, from the comparisons of thermokinetic parameters of non-isothermal and isothermal kinetic model simulation; and from the TBHP and TBEC kinetic parameters we could observe that the mechanism of thermal decomposition correspond to the autocatalytic reaction and the *n*th order, respectively, in this study.

The comparisons of the TBHP and TBEC DSC non-isothermal and isothermal tests of the experimental data and data derived from simulated *n*th order reaction and autocatalytic reaction for heat production versus time are shown in Figs. 3, 4, 5, 6 7, 8, 9, and 10, respectively. Although both the TBHP use of simulated autocatalytic kinetic models and the TBEC use of simulated *n*th order kinetic models, respectively and to match original DSC experimental data were proven to give superior results, not all of the data are compatible with the model.

Figure 4 shows that the heat effects of TBPH at the 4 and 6 °C min^{-1} scanning rates are greater than those observed at the other scanning rates. In addition, Fig. 7 shows that the heat effects of TBEC at the 1 and 6 °C min^{-1} scanning rates are greater than those observed at the other scanning rates. While analyzing the TBHP and TBEC's thermokinetic parameters by kinetic model simulation, we obtained two numbers for the autocatalytic thermokinetic parameters when using scanning rates of 1 and 2 °C min^{-1} and two numbers for the *n*th order thermokinetic parameters when using scanning rates of 2 and 4 °C min^{-1} in the thermal hazard simulation, respectively.

In this study, the TMR_{iso}, TER, and TCL of LOPs were acquired by simulating *n*th order and autocatalytic non-isothermal simulations, as displayed in Figs. 11, 12, 13, and 14. Figure 11 shows TMR_{iso} of TBHP obtained, values of which were ca. less than 30 °C and exceeded the upper limit of only 5 days, and shows the TER of TBHP immediately reaching the maximum energy release. Figure 12 shows the TCL of TBHP is less than 20 °C, which is beyond the upper limit of only 40 days.

Figure 13 shows TMR_{iso} of TBEC obtained, values of which were ca. less than 30 °C and exceeded the upper limit of only 5 days, and shows the TER of TBEC immediately reaching the maximum heat production. Figure 14 shows the TCL of TBHP is less than 30 °C, which is beyond the upper limit of only 25 days.

The analysis of thermokinetic parameters of the thermal decomposition of LOPs depended on the

Table 4 Comparisons TBHP of the thermokinetic parameters for the evaluation of *n*th order and autocatalytic models under non-isothermal condition

Scanning rate/°C/min	1		2		4		6	
Kinetic model	*N*-th order	Autocatalytic	*N*-th order	Autocatalytic	*N*-th order	Autocatalytic	*N*-th order	Autocatalytic
$\ln(k_0)$/ln/s	25.0949	21.0858	25.4198	22.7305	26.6397	20.7607	25.4393	21.0434
E_a/kJ/mol	107.8848	94.0886	108.5878	97.5149	112.1476	90.1680	108.2816	90.6882
Reaction order (n)/nth	0.7245	0.9005	0.7193	1.1190	0.7222	0.9578	0.7634	1.1492
Reaction order (n_1)/auto								
Reaction order (n_2)	N/A	0.6028	N/A	0.8599	N/A	0.5248	N/A	0.7345
Autocatalytic constant/z	N/A	0.4022	N/A	0.2632	N/A	0.1121	N/A	0.1680
ΔH_d/kJ/kg	898.6937	890.1324	1022.0498	1006.9481	761.2197	750.7822	876.7006	863.6956

Table 5 Comparisons TBHP of the thermokinetic parameters for the evaluation of *n*th order and autocatalytic models under isothermal condition

Isothermal temperature/°C	125		130		135		140	
Kinetic model	*N*-th order	Autocatalytic	*N*-th order	Autocatalytic	*N*-th order	Autocatalytic	*N*-th order	Autocatalytic
$\ln(k_0)$/ln/s	28.1751	22.1349	37.8305	22.0041	31.3871	22.6779	23.4791	22.4324
E_a/kJ/mol	114.6169	90.6747	148.7842	91.2516	126.6329	91.8571	105.0637	89.9320
Reaction order (n)/nth	0.7119	1.8338	0.8255	2.9860	0.6850	2.4752	0.2442	2.9877
Reaction order (n_1)/auto								
Reaction order (n_2)	N/A	0.5476	N/A	0.4582	N/A	0.7018	N/A	0.6320
Autocatalytic constant/z	N/A	1.376E−03	N/A	3.247E−04	N/A	1.591E−04	N/A	1.001E−08
ΔH_d/kJ/kg	706.6694	708.2880	583.4044	684.5263	787.6206	820.4815	371.6517	529.8774

Table 6 Comparisons TBEC of the thermokinetic parameters for the evaluation of *n*th order and autocatalytic models under non-isothermal condition

Scanning rate/°C/min	1		2		4		6	
Kinetic model	*N*-th order	Autocatalytic	*N*-th order	Autocatalytic	*N*-th order	Autocatalytic	*N*-th order	Autocatalytic
$\ln(k_0)$/ln/s	23.6729	24.2285	23.9840	27.6629	24.7125	22.8402	23.5361	29.8458
E_a/kJ/mol	103.2783	102.9039	103.7124	111.2674	105.3640	96.9755	101.5159	123.3809
Reaction order (n)/nth	0.6338	1.2002	0.6411	1.6449	0.6954	1.1446	0.6708	0.9508
Reaction order (n_1)/auto								
Reaction order (n_2)	N/A	0.7300	N/A	1.5518	N/A	0.7208	N/A	0.0893
Autocatalytic constant/z	N/A	0.2150	N/A	0.1713	N/A	0.2248	N/A	0.2258
ΔH_d/kJ/kg	844.9007	834.1474	918.7705	928.5947	900.7224	893.1634	945.6073	919.9869

reliability of the kinetic model. We applied the isothermal and non-isothermal kinetic models for the evaluation of thermokinetic parameters and compared the results with the simulated thermal analysis. This approach led to the development of a swift and precise procedure for the evaluation of thermal decomposition properties of LOPs.

Dewar vessel and 25-kg barrel package thermal hazard simulations

To simulate the thermal hazard of LOP, the critical parameters for the thermal hazard were determined numerically from the chemical kinetics for several types of reactor geometries and various boundary conditions,

Table 7 Comparisons TBEC of the thermokinetic parameters for the evaluation of *n*th order and autocatalytic models under isothermal condition

Isothermal temperature/ °C	120		125		130		135	
Kinetic model	*N*-th order	Autocatalytic	*N*-th order	Autocatalytic	*N*-th order	Autocatalytic	*N*-th order	Autocatalytic
$\ln(k_0)$/ln/s	23.3295	42.1710	23.4560	22.3777	23.7062	28.6159	23.7494	32.7945
E_a/kJ/mol	101.2264	165.3285	101.8804	96.7390	103.2252	116.1235	102.1790	129.5870
Reaction order (n)/*n*th	0.9270	0.9692	0.7655	1.2364	0.7111	1.6767	0.7088	1.6311
Reaction order (n_1)/auto								
Reaction order (n_2)	N/A	8.515E−03	N/A	0.2884	N/A	0.4693	N/A	0.6540
Autocatalytic constant/z	N/A	1.1964	N/A	0.0867	N/A	7.383E−03	N/A	0.0945
ΔH_d/kJ/kg	860.8048	823.6484	774.9810	777.9756	859.5601	875.1620	799.7425	808.7396

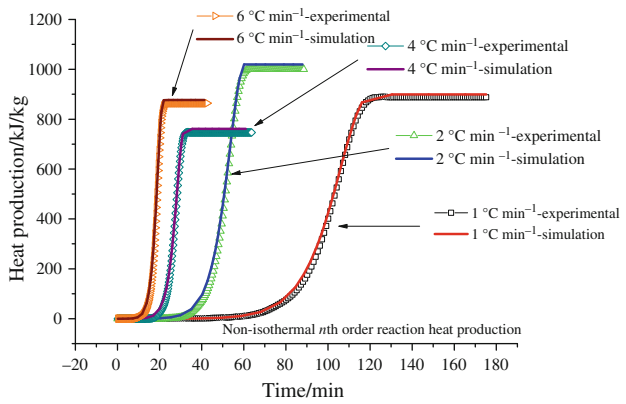

Fig. 3 TBHP heat production versus time curves of the *n*th order reaction with scanning rates of 1, 2, 4, and 6 °C min^{-1} by experiment and simulation

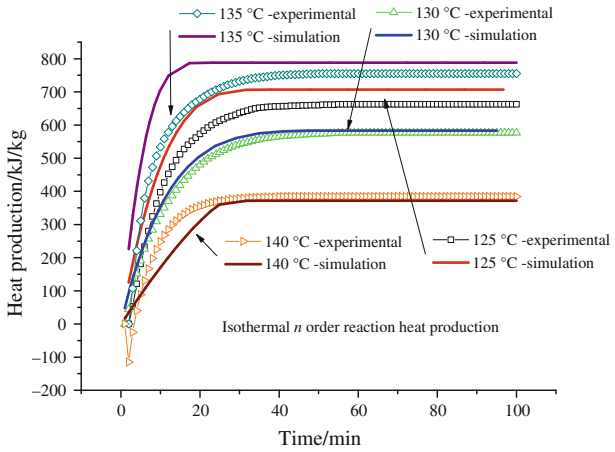

Fig. 5 TBHP heat production versus time curves of the experimental data and *n*th order reaction simulation with isothermal temperatures of 125, 130, 135, and 140 °C

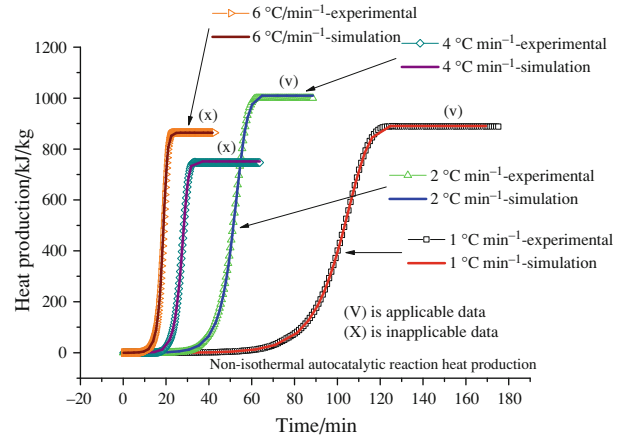

Fig. 4 TBHP heat production versus time curves of the autocatalytic reaction with scanning rates of 1, 2, 4, and 6 °C min^{-1} by experiment and simulation

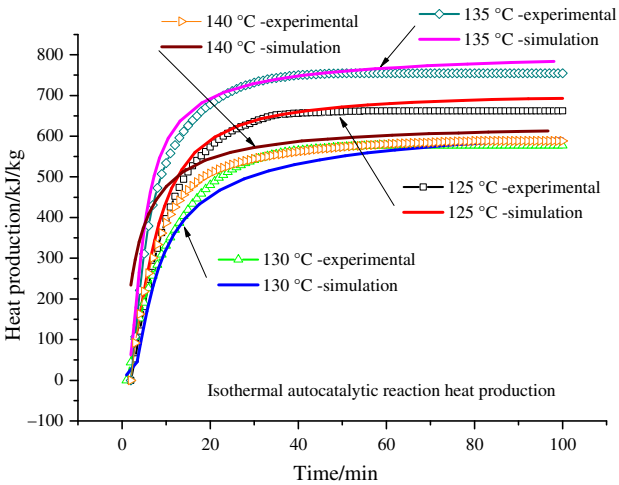

Fig. 6 TBHP heat production versus time curves of the experimental data and autocatalytic simulation with isothermal temperatures of 125, 130, 135, and 140 °C

including the possibility of setting boundary shells. For liquid thermal hazard simulations, the following statements were used [9, 10]:

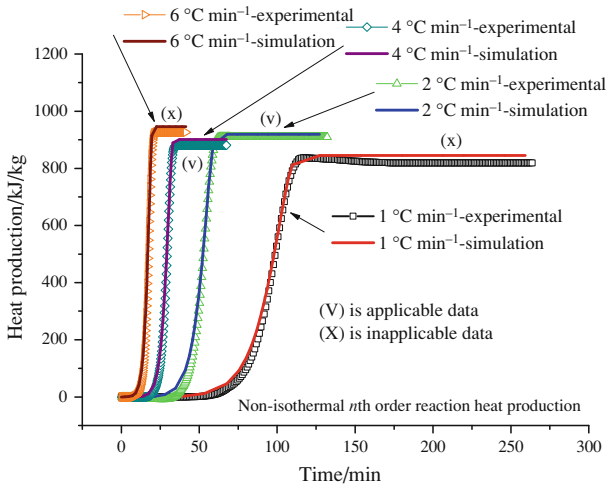

Fig. 7 TBEC heat production versus time curves of the *n*th order reaction with scanning rates of 1, 2, 4, and 6 °C min^{-1} by experiment and simulation

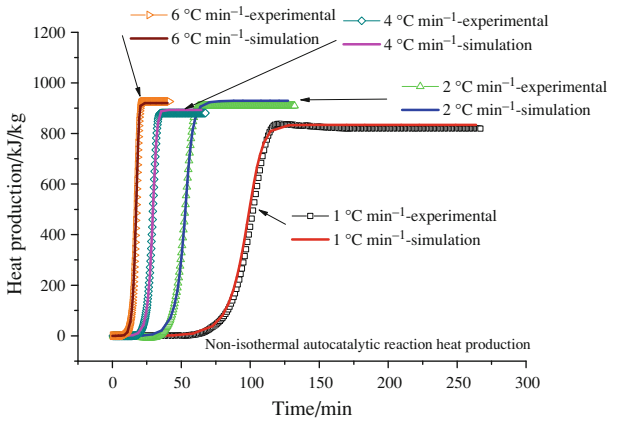

Fig. 8 TBEC heat production versus time curves of the autocatalytic reaction with scanning rates of 1, 2, 4, and 6 °C min^{-1} by experiment and simulation

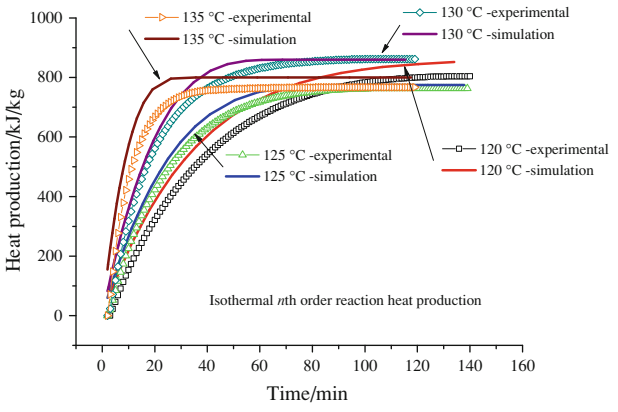

Fig. 9 TBEC heat production versus time curves of the experimental data and autocatalytic simulation with isothermal temperatures of 125, 130, 135, and 140 °C

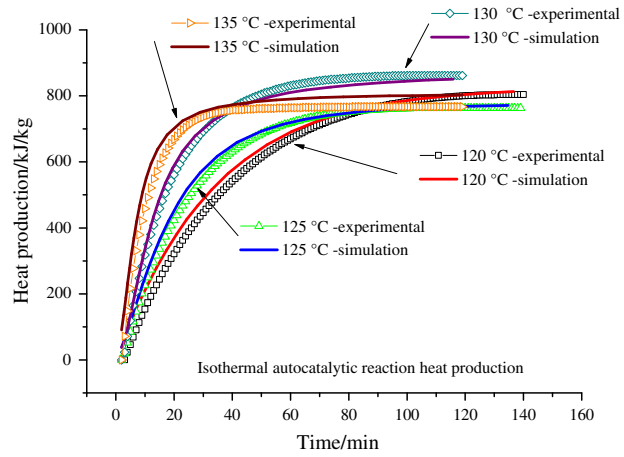

Fig. 10 TBEC heat production versus time curves of the experimental data and autocatalytic simulation with isothermal temperatures of 125, 130, 135, and 140 °C

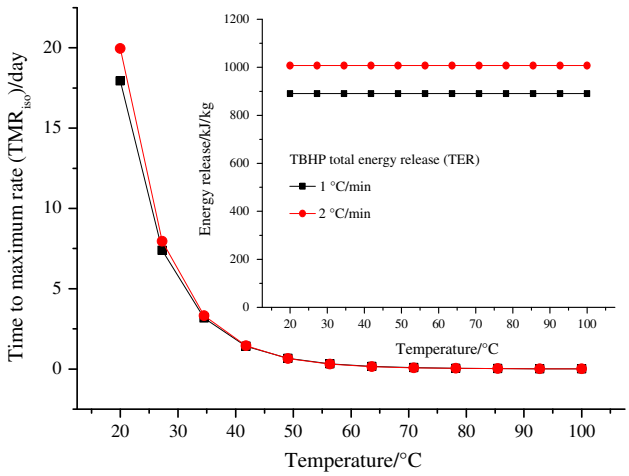

Fig. 11 Total energy release under isothermal conditions of the thermal decomposition of TBHP and the time until the maximum rate were achieved at scanning rates of 1 and 2 °C min^{-1}

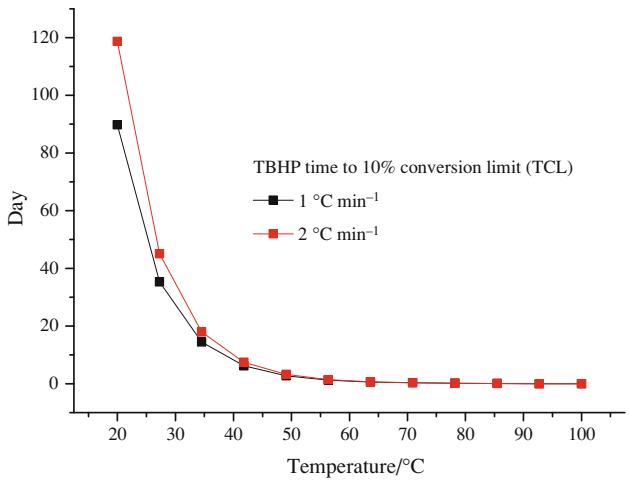

Fig. 12 Simulated TBHP time until 10% conversion at scanning rates of 1 and 2 °C min^{-1}

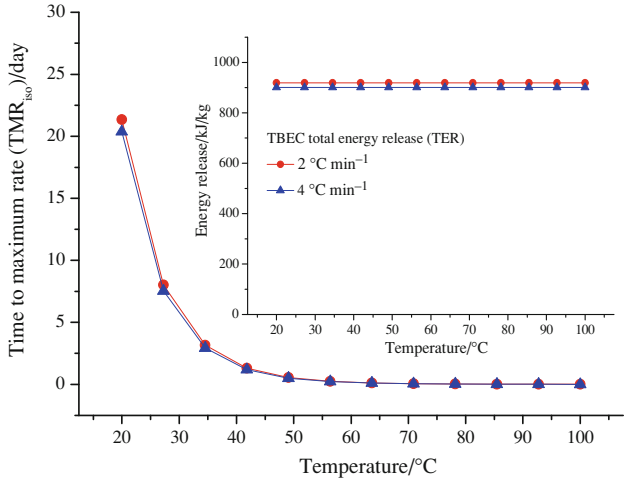

Fig. 13 Total energy release under isothermal conditions of the thermal decomposition of TBEC and the time until the maximum rate were achieved at scanning rates of 2 and 4 °C min^{-1}

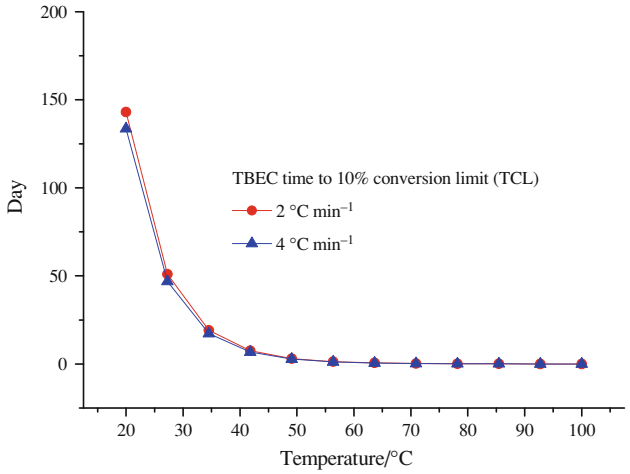

Fig. 14 Simulated TBEC time until 10% conversion at scanning rates of 2 and 4 °C min^{-1}

$$\rho C_P \frac{\partial T}{\partial t} = div(\lambda \Delta T) + W \quad (6)$$

Thermal conductivity equation

$$\frac{\partial \alpha_i}{\partial t} = r_i \quad i = 1, \ldots NC \quad (7)$$

Kinetic equations (formal models)

$$W = \sum_{(i)} Q_i^{\infty} r_i \quad \text{Heat power equation} \quad (8)$$

where T is the temperature, t is the time, ρ is the density, C_P is the specific heat, λ is the heat conductivity, Q_i^{∞} is the reaction calorific effect, W is the heat power, r is the reaction rate constant, α is the degree of conversion for a component, NC is the number of components, and i is the component number.

The initial fields for the temperature and the conversions were constant throughout the reactor volume [9, 10]:

$$\begin{aligned} \mathrm{T}|_{t=0} &= \mathrm{T}_0 \\ \alpha_i|_{t=0} &= \alpha_{i0} \end{aligned} \quad (9)$$

The index 0 indicates the initial values of the temperature and conversion.The boundary conditions of the first, second, and third kind were specified as [9, 10]

$$\text{1st kind: } \mathrm{T}|_{\text{wall}} = \mathrm{T}_e(t) \quad \text{Temperature} \quad (10)$$

$$\text{2nd kind: } q|_{\text{wall}} = q(t) \quad \text{Heat flow} \quad (11)$$

$$\text{3rd kind: } -\lambda \left.\frac{\partial T}{\partial n}\right|_s = \chi(\mathrm{T}_{\text{wall}} - \mathrm{T}_{\text{e}}) \quad \text{Newton's cooling law} \quad (12)$$

The indices "wall" and "e" relate to the parameters on the boundary and the environment, respectively; q is the heat flow, and n is the unit outer normal on the boundary.

The results of the thermal hazard simulation for the SADT, CT, ET, and TCR are presented in Table 8. The thermal decomposition stability of 0.5-L Dewar vessels was greater than that of the 25-kg barrel package. The

Table 8 The thermal hazard simulations for SADT, CT, ET, and TCR in the 0.5-L Dewar vessel and 25-kg barrel package

Sample	Size	Scanning rate/°C/min	SADT/°C in literature	SADT/°C	CT/°C	ET/°C	TCR/°C
TBHP	0.5-L	1	>60[a]	52	42	47	52.32
		2		52	42	47	51.34
	25-kg	1	NA	44	34	39	44.15
		2		44	34	39	43.43
TBEC	0.5-L	2	60[b]	54	44	49	53.74
		4		53	43	48	53
	25-kg	2	NA	46	36	41	45.79
		4		46	36	41	44.83

[a] Syrgis [4]

[b] Pergan [5]

stability and applicability worsened as the reactor size increased. The results of thermal hazard simulation also proved that the smaller size container has a better beneficial exothermal effect for the containment of LOPs than a huge package.

We developed a swift thermal analysis technology to determine the thermokinetic parameters and the thermal hazard of LOPs. These results could be applied toward energy reduction and safer designs for use and in storage. In addition to analyzing the thermal decomposition kinetic parameters through comparing the non-isothermal and isothermal kinetic model simulations, we found that the results presented a reasonable model to enable calculation of the kinetic parameters of thermal decomposition. The validity of the results significantly depends on the reliability of the applied kinetic model, which can be validated by the proper selection of a kinetic model for a reaction, and the correctness of the methods used for the kinetics evaluation. The model can be applied to evaluating other organic peroxides or chemicals.

Conclusions

The thermokinetic parameters and thermal hazard of LOPs were studied using non-isothermal and isothermal kinetic models of thermal decomposition. Modeling the thermokinetic and the safety parameters provided precise hazard information concerning the avoidance of thermal accidents during process manufacturing, storage and transportation. We developed a beneficial analysis model for the thermokinetic and thermal hazard parameters of LOPs with the swift thermal analysis technology.

Acknowledgements The authors are indebted to the donors of the National Science Council (NSC) in Taiwan under the contract number NSC 100-2218-E-468-001- for financial support. In addition, the authors are grateful to ACE Chemical Corp. Taiwan, ROC.

References

1. European agreement concerning the international carriage of dangerous goods by road (ADR). New York: United Nations; 2009.
2. Recommendations on the transport of dangerous goods, manual of tests and criteria. 4th ed. New York: United Nations; 2003.
3. Recommendations on the transport of dangerous goods, model regulations. 16th ed. New York: United Nations; 2009.
4. Material Safety Data Sheet, Syrgis Performance Initiators Inc., 334 Phillips 311 Rd., Helena, AR 72342, 2007.
5. Material Safety Data Sheet, PERGAN GmbH, Schlavenhorst 71, D-46395 Bocholt, 2010.
6. Lin CP, Chang YM, Tseng JM, Shu CM. Comparisons of *n*th order kinetic algorithms and kinetic model simulation on HMX by DSC tests. J Therm Anal Calorim. 2010;100(2):607–14.
7. Lin CP, Tseng JM, You ML, Chu YC, Shu CM. Modeling thermal decomposition kinetic algorithm on CL-20 and HMX. Inter J Chem React Eng. 2010;8:A146.
8. Tsai LC, Wei JM, Chu YC, Chen WT, Tsai FC, Shu CM, Lin CP. RDX kinetic model evaluation by nth order kinetic algorithms and model simulations. Adv Mater Res. 2011;189–193:1413–6.
9. Lin CP, Tseng JM, Chang YM, Liu SH, Shu CM. Modeling liquid thermal explosion reactor containing tert-butyl peroxybenzoate. J Therm Anal Calorim. 2010;102:587–95.
10. Lin CP, Chang CP, Chou YC, Chu YC, Shu CM. Modeling solid thermal explosion containment on reactor HNIW and HMX. J Hazard Mater. 2010;176:549–58.
11. Steensma M, Schuurman P, Malow M, Krause U, Wehrstedt KD. Evaluation of validity of the UN SADT H.4 test for solid organic peroxides and self-reactive substances. J Hazard Mater. 2005; A117:89–102.
12. Malow M, Michael-Schulz H, Wehrstedt KD. Evaluative comparison of two methods for SADT determination (UN H.1 and H.4). J Loss Prev Process Ind. 2010;23:740–4.
13. Malow M, Wehrstedt KD. Prediction of the self-accelerating decomposition temperature (SADT) for solid organic peroxides from differential scanning calorimetry (DSC) measurements. J Hazard Mater. 2005;A120:21–4.
14. Fisher HG, Goetz DD. Determination of self-accelerating decomposition temperatures using the accelerating rate calorimeter. J Loss Prev Process Ind. 1991;4:305–16.
15. Fisher HG, Goetz DD. Determination of self-accelerating decomposition temperatures for self-reactive substances. J Loss Prev Process Ind. 1993;6(3):183–94.
16. Li YF, Hasegawa K. On the thermal decomposition mechanism self-accelerating materials and evaluating method for their SADTs. Barcelona: 9th International Symposium Loss Prevention in the Process Industries; 1998, p. 555–569.
17. Sun JH, Li YF, Hasegawa K. A study of self-accelerating decomposition temperature (SADT) using reaction calorimetry. J Loss Prev Process Ind. 2001;14(5):331–6.
18. Whitmore MW, Wilberforce JK. Use of the accelerating rate calorimeter and the thermal activity monitor to estimate stability temperatures. J Loss Prev Process Ind. 1993;6(2):95–101.
19. Wilberforce JK. The use of the accelerating rate calorimeter to determine the SADT of organic peroxides. Texas: Columbia Scientific Corp. Internal report; 1981.
20. Yang D, Koseki H, Hasegawa K. Predicting the self-accelerating decomposition temperature (SADT) of organic peroxides based on non-isothermal decomposition behavior. J Loss Prev Process Ind. 2003;16(5):411–6.
21. Yu YH, Hasegawa K. Derivation of the self-accelerating decomposition temperature for self-reactive substances using isothermal calorimetry. J Hazard Mater. 1996;45(2–3):193–205.
22. Frank-Kamenetskii D. Diffusion and heat exchange in chemical kinetics. 2nd ed. New York: Plenum Press; 1969.